End-to-End Distribution Function of Two-Dimensional Stiff Polymers for all Persistence Lengths

B. Hamprecht[1], W. Janke[2] and H. Kleinert[1]

[1] *Institut für Theoretische Physik, Freie Universität Berlin,*
Arnimallee 14, D-14195 Berlin, Germany
[2] *Institut für Theoretische Physik, Universität Leipzig,*
Augustusplatz 10/11, D-04109 Leipzig, Germany
e-mail: bodo.hamprecht@physik.fu-berlin.de e-mail: wolfhard.janke@itp.uni-leipzig.de e-mail: hagen.kleinert@physik.fu-berlin.de

We set up and solve a recursion relation for all even moments of a two-dimensional stiff polymer (Porod-Kratky wormlike chain) and determine from these moments a simple analytic expression for the end-to-end distribution applicable for all persistence lengths.

I. INTRODUCTION

In a recent note [1], two of us found a new recursion relation for the even moments of the end-to-end distribution of stiff polymers in D dimensions and used the resulting moments of high order to construct an simple analytic distribution function for the end-to-end distance $r = R/L$. For large reduced persistence lengths ξ/L, the result agrees well with perturbative and Monte Carlo results of Wilhelm and Frey [2], for smaller ξ/L with the random chain distribution including the weak-stiffness corrections of Ref. [3].

Recently, Dahr and Chaudhuri [4] have pointed out the existence of an interesting dip structure in for two dimensions at intermediate ξ-values if one plots the radial distribution density $p(\xi, r) \equiv P(\xi, r)/r$ with the normalization $\int_0^1 r\, dr\, p(\xi, r) = 1$. In the usual plots of $P(\xi, r)$, this feature is hidden by the extra r-factor. It is interesting to see how this dip can be accommodated by a simple analytic approximation of the type found in Ref. [1]. The three parameters used in the three-dimensional plots will obviously not be sufficient to reproduce the dip. In this paper we solve this problem and find an analytic expression which fits excellently high-precision Monte Carlo data using the even moments obtained in Ref. [5–7] in D dimensions. To make this paper self-contained we briefly summarize the derivation.

The end-to-end distribution function of a stiff polymer in two dimensions is given by the path integral [7]

$$P_L(\mathbf{R}) \propto \int d\theta_b\, d\theta_a \mathcal{D}\theta(s) e^{-E_b/k_B T} \delta^{(2)}\left(\mathbf{R} - \int_0^L ds\, \mathbf{u}(s)\right) \tag{1.1}$$

with the bending energy

$$E_b = \frac{\kappa}{2} \int_0^L ds\, [\mathbf{u}'(s)]^2, \tag{1.2}$$

where $\mathbf{u}(s) = (\cos\theta(s), \sin\theta(s))$ are the direction vectors of the polymer links, and κ is the stiffness which defines the persistence length $\xi \equiv 2\kappa/k_B T$. Due to the presence of the δ-function in the integrand, the path integral is not exactly solvable. It is, however, easy to find arbitrarily high even moments for the radial distribution of the end-to-end distribution. The interesting dip structure is observed in the radial distribution $p(R/L) \equiv P_L(\mathbf{R}) \cdot L/R$. In the sequel, we shall emphasize the stiffness dependence of $p(R/L)$ by including ξ/L in the argument and discussing $p(\xi/L, R/L)$. For brevity, we shall also go to natural length units where $L = 1$. The even moments of the end-to-end distribution are then given by the integrals

$$\langle R^{2n} \rangle \equiv \int_0^1 dr\, r^{2n+1}\, p(\xi, r). \tag{1.3}$$

These moments can be obtained from the coefficient of $\lambda^{2n}/2^{2n}(2n)!$ in the expansion, in powers of λ, of an integral

$$f(\tau; \lambda) \equiv \int_0^\pi d\theta\, \psi(\theta, \tau; \lambda), \tag{1.4}$$

evaluated at the euclidean time $\tau = \xi$. The wave function $\psi(\theta, \tau; \lambda)$ is a solution of the Schrödinger equation on the circle in euclidean time with a potential $V(\theta) = (\lambda/2)\cos\theta$ (see Refs. [5–7]):

$$\hat{H}\psi(\theta, \tau; \lambda) = -\frac{d}{d\tau}\psi(\theta, \tau; \lambda), \tag{1.5}$$

where

$$\hat{H} = -\frac{1}{2}\frac{d^2}{d\theta^2} + \frac{1}{2}\lambda\,\cos\theta. \tag{1.6}$$

II. RECURSIVE SOLUTION OF THE SCHROEDINGER EQUATION.

The function $f(L; \lambda)$ has a spectral representation

$$f(L; \lambda) \equiv \sum_{l=0}^\infty \frac{\int_0^\pi d\theta\, \varphi^{(l)\dagger}(\theta) \exp\left(-E^{(l)} L\right) \varphi^{(l)}(0)}{\int_0^\pi d\theta\, \varphi^{(l)\dagger}(\theta)\, \varphi^{(l)}(\theta)}, \tag{2.1}$$

where the $\varphi^{(l)}(\theta)$ are arbitrarily normalized eigensolutions of the time-independent interacting Schrödinger equation $\hat{H}\varphi^{(l)}(\theta) = E^{(l)}\varphi^{(l)}(\theta)$. We calculate these by perturbation theory, starting from the eigenstates $|l\rangle$ of

the unperturbed Hamiltonian $\hat{H}_0 = -(1/2)d^2/d\theta^2$, with eigenvalues $E_0^{(l)} = l^2/2$. The associated Schrödinger wave functions $\varphi^{(l)}(\theta) = \langle\theta|l\rangle$ are $\varphi^{(0)}(\theta) = 1/\sqrt{4\pi}$ and $\varphi^{(l)}(\theta) = \cos(l\theta)/\sqrt{\pi}$. Note that the ground state wave function is not normalized to unity on purpose, for later convenience. Now we set up a recursion scheme for the expansion coefficients $\gamma_{l',i}^{(l)}$ and $\epsilon_j^{(l)}$ of the eigenfunctions and their energies:

$$|\varphi^{(l)}\rangle = \sum_{l',i=0}^{\infty} \gamma_{l',i}^{(l)}\, \lambda^i\, |l'\rangle, \quad E^{(l)} = \sum_{j=0}^{\infty} \epsilon_j^{(l)}\, \lambda^j. \quad (2.2)$$

The procedure is described in [1, 8]. The properties of the unperturbed system determine the initial conditions at $\lambda = 0$ for the recursion:

$$\gamma_{l,i}^{(l)} = \delta_{i,0}, \qquad \gamma_{k,0}^{(l)} = \delta_{l,k}, \qquad \epsilon_0^{(j)} = j^2/2. \quad (2.3)$$

To proceed, we need the the matrix elements of the perturbing Hamiltonian $\hat{H}_I$ in the unperturbed basis, which are simply $\langle n|\hat{H}_I|n1\rangle = \lambda/2$. Inserting the expansions (2.2) into the Schrödinger equation (1.5), projecting the result onto some base vector $\langle k|$, and extracting the coefficient of λ^i, we obtain the following recursion relations:

$$\epsilon_i^{(0)} = \gamma_{1,i-1}^{(0)}, \qquad \epsilon_i^{(l)} = (\gamma_{l+1,i-1}^{(l)} + \gamma_{l-1,i-1}^{(l)})/2, \quad (2.4)$$

and

$$\gamma_{0,i}^{(l)} = \frac{2}{l^2}\left(\gamma_{1,i-1}^{(l)} - \sum_{j=1}^{i-1}\epsilon_j^{(l)}\gamma_{0,i-j}^{(l)}\right), \qquad (2.5)$$

$$\gamma_{k,i}^{(l)} = \frac{1}{l^2-k^2}\left(\gamma_{k+1,i-1}^{(l)} + \gamma_{k-1,i-1}^{(l)} - 2\sum_{j=1}^{i-1}\epsilon_j^{(l)}\gamma_{k,i-j}^{(l)}\right). \quad (2.6)$$

Starting from the initial values (2.3), these recursion relations determine successively the higher-order expansion coefficients in (2.2). Inserting the resulting expansions (2.2) into Eq. (2.1), only the constant parts in $\varphi^{(l)}(\theta)$ which are independent of θ will survive the integration in the numerators. Therefore $\varphi^{(l)}(\theta)$ in the numerators of (2.1) may be replaced by the constants:

$$\varphi_{\mathrm{symm}}^{(l)} \equiv \int_0^{2\pi} d\theta\, \varphi^{(0)\dagger}(\theta)\varphi^{(l)}(\theta) = \frac{1}{2}\sum_{i=0}^{\infty}\gamma_{0,i}^{(l)}\lambda^i, \quad (2.7)$$

the factor $1/2$ reflecting the special normalization of $\varphi^{(0)}(\theta)$. The denominators of (2.1) become explicitly

$$\int_0^{\pi} d\theta\, \varphi^{(l)\dagger}(\theta)\,\varphi^{(l)}(\theta) = \sum_i\left(|\gamma_{0,i}^{(l)}|^2/2 + \sum_{l'}|\gamma_{l',i}^{(l)}|^2\right)\lambda^{2i}, \quad (2.8)$$

where the sum over i is limited by the power of λ^2 up to which we want to carry the perturbation series; also l' is restricted to a finite number of terms, because of a band-diagonal structure of the $\gamma_{l',i}^{(l)}$ (see [1]). Extracting the coefficients of the power expansion in λ from (2.1) we obtain all desired moments of the end-to-end distribution, the lowest two being well-known:

$$\langle R^2 \rangle = 2\left\{\xi - \xi^2\left[1 - e^{-1/\xi}\right]\right\}, \qquad (2.9)$$

$$\langle R^4 \rangle = 8\xi^2 - \xi^3\left(30 + \frac{40}{3}e^{-1/\xi}\right)$$
$$+ \xi^4\left(\frac{87}{2} - \frac{392}{9}e^{-1/\xi} + \frac{1}{18}e^{-4/\xi}\right). \qquad (2.10)$$

The calculation of higher moments can easily be done with the help of a Mathematica program, which we have placed on the internet in notebook form [9]. The above lowest moments agree with those in Ref. [4].

III. END-TO-END DISTRIBUTION AND COMPARISON WITH MONTE CARLO DATA

As in the previous paper, we shall now set up an analytic distribution function for $p(\xi, r)$. In order to be able to accommodate the dip structure, we must allow for an extra polynomial factor as compared to the simple ansatz in [1]:

$$p(\xi, r) = (a_0 + a_2\, r^2 + a_4\, r^4 + a_6\, r^6)\, r^k\, (1 - r^\beta)^m. \quad (3.1)$$

The parameters are determined to incorporate optimally our knowledge of the exact moments according to equation 1.3. The coefficients $a_0, \ldots, a_6$, k, β, m are functions of ξ and are determined by forcing the moments of (3.1) to fit the exact moments in the range $0 \leq n \leq \mathrm{Max}(6, 10\,\xi)$. For $\xi < 1$, best results are obtained with the parameter $k = 0$. A comparison of $p(\xi, r)$ with Monte-Carlo data is shown in Figs. 1 and 2. The associated coefficients are listed in Table I. The calculation of the coefficients in (3.1) requires some care to guarantee sensitivity to possible local minima, and to avoid running into unphysical oscillations. The latter may arise from the existence of polynomials in which all moments lower than some n vanish. Such oscillations are avoided by controlling the high moments and using only low polynomial coefficients in (3.1). A more involved strategy is necessary to avoid low-quality local solutions. We proceed as follows:

- In a first step we set $a_2 = a_4 = a_6 = 0$, $\beta = 2$, and determine preliminary values for k and m by fitting two higher moments of n near $20\,\xi$. The first coefficient a_0 is fixed by normalization. This gives a reasonable starting value for m.

ξ	a_0	a_2	a_4	a_6	k	m	β
.0025	400.0	0	0	0	0	196.784	1.99496
.01	100.0	0	0	0	0	47.5378	1.98197
.02	50.0	0	0	0	0	22.9930	1.97564
.033	29.5302	−58.9195	77.9373	−87.3526	0	12.0224	2.00505
.067	14.0952	−29.8504	66.8842	−68.1985	0	5.62896	2.21169
.1	9.20629	−34.7515	50.6223	−26.2289	0	13.2737	10.5486
.2	4.18239	−7.45808	11.616	−7.30855	0	10.2031	16.6444
.25	3.12655	−4.9930	13.1086	−10.0222	0	9.42195	20.0750
.3	2.38054	−3.38168	12.8823	−9.51483	0	9.16782	23.0164
.35	1.82132	−2.062292	11.2343	−7.24306	0	8.84230	25.5206
.4	1.39171	−0.952158	8.94986	−4.33545	0	8.49552	27.9120
.5	0.800939	0.647524	4.36711	1.36933	0	8.06681	33.2814
1	42.8376	−173.308	263.327	−123.515	4.9880	11.4933	85.8428
2	504.624	−1832.52	2271.51	−925.829	13.4792	30.4949	244.143

TABLE I: Coefficients of the analytic distribution function for $p(\xi, r)$ in Eq. (3.1) for various values of the persistence length ξ. They are obtained by making six or seven even moments of $p(\xi, r)$ agree with the exact ones.
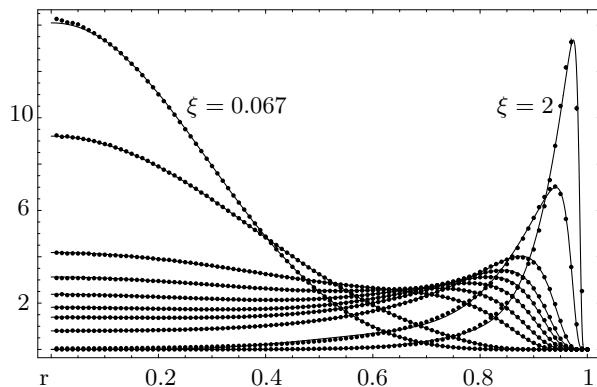

FIG. 1: End-to-end distribution $p(\xi, r)$ in $D = 2$ dimensions as a function of r for various values of the reduced persistence length $\xi = 0.067, .1, .2, .25, .3, .35, .4, .5, 1, 2$. The solid curves show the model functions (3.1) with parameters from modelI. The dots represent Monte Carlo data.
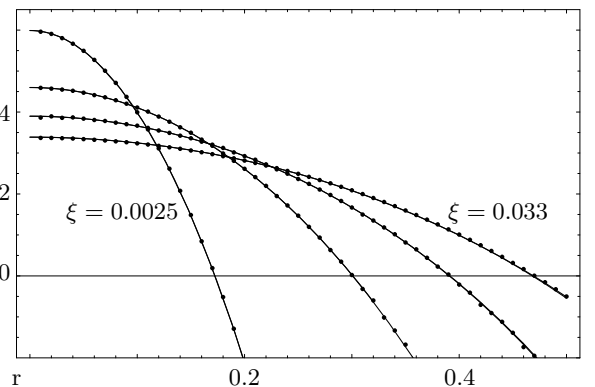

FIG. 2: End-to-end distribution $\log p(\xi, r)$ in $D = 2$ dimensions as a function of r for various values of the reduced persistence length for very sloppy polymers with $\xi = 0.0025, .01, .02, .033$. The solid curves show the model functions (3.1) with parameters from Table I. In this range they fall on top of the curves from the Daniels approximation (3.2) within the accuracy of the plot. The dots represent Monte Carlo data.

- In a second step, we introduce one more of the higher moments to improve the solution for k, m, and β.

- Next we solve for the coefficients a_j by bringing yet more moments into play. If $\xi < 1$, we take $k = 0$ and solve for the a_j, keeping β and m fixed, based on four properly chosen moments. Then we solve for β and m keeping the a_j fixed, based on a choice of two moments. This alternating procedure is repeated three times. Finally, we solve for the a_j, β, and m simultaneously, based on six properly chosen moments.

- For $\xi \geq 1$, we proceed similarly, but allow for $k \neq 0$. The search for good coefficients a_j alternating with a search for good k, β, and m is repeated until it converges. Unlike before we make no further attempt to solve for all seven parameters simultaneously.

There are two simple approximations of the radial distribution $p(\xi, r)$. One is derived for small ξ by Daniels

[3, 7], which reads in $D = 2$ dimensions:

$$p(\xi, r) = \exp\left(\frac{-r^2}{\xi}\right)\left[\frac{1}{\xi}\left(1 + \frac{5}{4}r^2\right) - \frac{7}{32\xi^2}r^4 - \frac{3}{4}\right].$$
(3.2)

At the origin, it has the nonzero value

$$p(\xi, 0) = 1/\xi - 3/4.$$
(3.3)

The other approximation is derived for large ξ [2, 7]:

$$p(\xi, r) \propto \frac{e^{-1/8\xi(1-r)}}{\xi^{5/4}(1-r)^{5/4}} U\left(\frac{-3}{4}, \frac{1}{2}, \frac{1}{8\xi(1-r)}\right), \quad (3.4)$$

where $U(a, b, z)$ is Kummer's confluent hypergeometric function.

In Fig. 3.3 we see, that our model function (3.1) reproduced very well the threshold values (3.3) for small ξ. In fact, the approximation 3.3 describes the behavior of the polymer at the sloppy end extremely well, with an accuracy comparable to that of (3.1). Deviations become visible only for $\xi \geq 0.1$ as demonstrated in Fig. 4.

The large-stiffness approximation (3.4), on the other hand, which is of course very good for large stiffness, is no longer acceptable for moderate $\xi \leq 2$, where our approximation is much better as shown in Fig. 5.

For $\xi > 2$, the computational effort fo fix the parameters in our model becomes somewhat large, so that in this range the approximation (3.4) is more useful than ours. In the intermediate region for $0.1 < \xi < 1$, however, both approximation schemes are far inferior to our model, which reproduces Monte Carlo data with high accuracy, as can be seen in Fig. 6.

In addition we check the quality of our simple distri-

FIG. 4: End-to-end distribution $p(\xi, r)$ for polymers in $D = 2$ dimensions as a function of r for various values of the reduced persistence length ξ in the moderately sloppy regime of $\xi = 0.1, 0.2, 0.3$. Solid curves show our model functions (3.1) with parameters from Table I fitting very well the Monte Carlo data (heavy dots). Dotted curves show the small-ξ Daniels approximation (3.2), which deviate strongly from data points. Dashed curves are large-stiffness approximation (3.4), which are just as bad.

FIG. 5: End-to-end distribution $p(\xi, r)$ for polymers in $D = 2$ dimensions as a function of r in the range of large reduced persistence length ξ for $\xi = 0.4, 0.5, 1, 2$. The solid curves show the model functions (3.1) with parameters from Table I. Heavy dots represent Monte Carlo data and dashed curves the large stiffness approximations (3.4). In this range our model function is still much better than both approximations. However, for $\xi > 2$ the computational effort may become so large, that the large-stiffness approximation is useful.
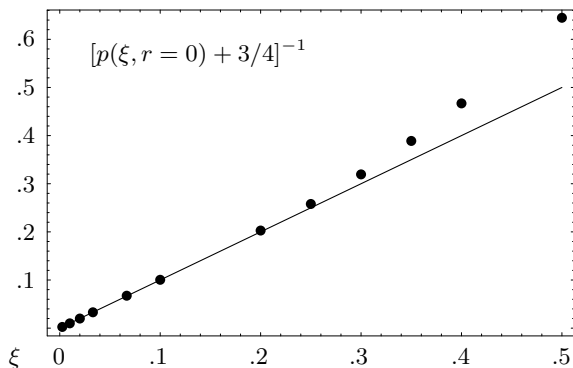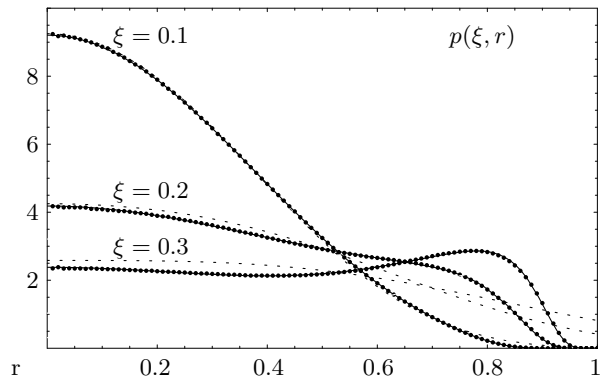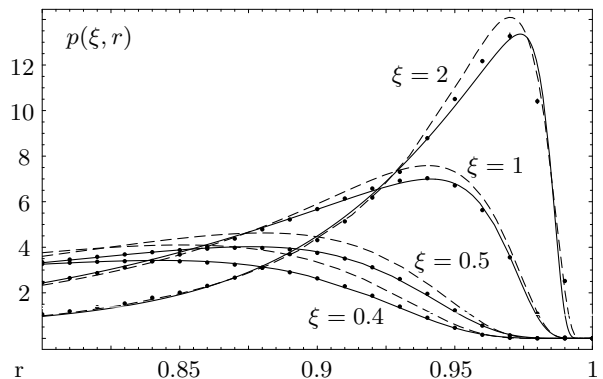

FIG. 3: Threshold values of the end-to-end distribution function $p(\xi, r = 0)$ for polymers in two dimensions as a function of the reduced persistence length ξ (dots) are compared to the approximate result 3.3 for sloppy chains with small values of ξ (straight line).

bution function (3.1) with the parameters of Table I by calculating its moments and comparing them with the exact ones. The comparison is shown in Table II for a large range of the persistence length ξ. As a measure of the quality of the approximation we use the quantity Σ,
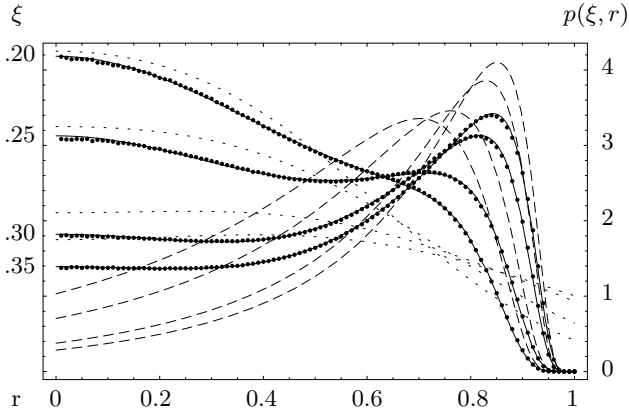
FIG. 6: End-to-end distribution $p(\xi, r)$ for polymers in $D = 2$ dimensions as a function of r for various values of the reduced persistence length in a medium range of $\xi = 0.2, 0.25, 0.3, 0.35$. The solid curves show the model functions (3.1) with parameters from Table I. Heavy dots show the Monte Carlo data, dotted curves represent the Daniels approximation (3.2), dashed curves the stiffness approximations (3.4). In this range our model function is far superior to any of the other two approximations and it is in addition valid for all radii. The $\xi = 0.25$ -curve shows the interesting dip structure.

listed in the second column of Table II, which sums up all squared deviations of the moments of the model from the exact ones in a relevant range of ξ:

$$\Sigma(\xi) = \sqrt{\sum_{n=0}^{N} \left[\langle R^{2n} \rangle_{\text{model}} - \langle R^{2n} \rangle_{\text{exact}} \right]^2}, \qquad (3.5)$$

where we have extended the sum over the moments up to the order of $N = 12$ for $\xi < 0.2$, and up to $N = 24$ for $\xi \geq 0.2$.

Let us also convince ourselves quantitatively of the high accuracy of our Monte Carlo data for the end-to-end distribution in Fig. (1) by listing the maximal deviation

$$\Delta_{\text{abs}} = \sup_{n=0}^{\infty} \left| \langle R^{2n} \rangle_{\text{MC}} - \langle R^{2n} \rangle_{\text{exact}} \right| \qquad (3.6)$$

of its moments, as well as the relative deviation

$$\Delta_{\text{rel}}(N_{\text{max}}) = \sup_{n=0}^{N_{\text{max}}} \left| \langle R^{2n} \rangle_{\text{MC}} / \langle R^{2n} \rangle_{\text{exact}} - 1 \right| \qquad (3.7)$$

up to the moment N_{max}. It is noteworthy that in spite of the simplicity of the model, it is a nontrivial task to

obtain accurate Monte Carlo results for $p(\xi, r)$ near $r = 0$ which are sensitively displayed in the plots of Fig. (1) but which are almost ignored by the moments. The reason for this difficulty is that the configuration space for the small-r data is very small and the binning of the data to estimate the density $p(\xi, r)$ is done on the r axis. One is caught in the competition between large systematic errors resulting from a necessarily large bin size Δr, and statistical errors from a too small Δr. As a compromise we employed in our simulations a uniform bin size $\Delta r = 0.01$ which in combination with a single-cluster update procedure and a statistics of 10^8 sampled chains yields a satisfactory accuracy near $r = 0$.

ξ	Σ	Δ_{abs}	$\Delta_{\text{rel}}(N_{\text{max}})$
.0025	3×10^{-12}	0.000 126	0.9%(16)
.01	2×10^{-13}	0.000 033	8%(16)
.02	1×10^{-10}	0.000 071	1%(16)
.033	5×10^{-9}	0.000 717	8%(16)
.067	2×10^{-6}	0.000 057	0.9%(16)
.1	5×10^{-5}	0.000 038	0.8%(24)
.2	4×10^{-5}	0.000 048	0.5%(24)
.25	9×10^{-5}	0.000 048	0.4%(24)
.3	13×10^{-5}	0.000 047	0.3%(24)
.35	2×10^{-4}	0.000 087	0.8%(36)
.4	2×10^{-4}	0.000 100	0.8%(36)
.5	2×10^{-4}	0.000 139	0.8%(36)
1	2×10^{-4}	0.000 217	0.4%(48)
2	8×10^{-5}	0.004 705	1.6%(48)

TABLE II: To illustrate the accuracy of our analytic approximation (3.1) of the end-to-end distribution we list the quantity Σ of Eq. (3.5) which measures the deviation of the even moments from the exact ones. The other two columns show the accuracy of the Monte Carlo data for the end-to-end distribution by listing the maximal deviation Δ_{abs} of its moments and the relative deviation $\Delta_{\text{rel}}(N_{\text{max}})$ up to the moment N_{max}.

[1] B. Hamprecht and H. Kleinert, *End-To-End Distribution Function of Stiff Polymers for all Persistence Lengths,* cond-mat/0305226.

[2] J. Wilhelm and E. Frey, Phys. Rev. Lett. **77**, 2581 (1996).

[3] H.E. Daniels, Proc. Roy. Soc. Edinburgh **63A**, 29 (1952). For details see also Chapter 15 of the textbook [7].

[4] A. Dhar and D. Chaudhuri, Phys. Rev. Lett **89**, 065502 (2002).

[5] H. Yamakawa, *Modern Theory of Polymer Solution*, Harper and Row, New York, 1971; *Helical Worrmlike Chains in Polymer Solution*, Springer, Berlin, 1997.

[6] G.S. Chirikjian and Y. Wang, Phys Rev E **62**, 880, (2000).

[7] H.Kleinert, *Path Integrals in Quantum Mechanics, Statistics and Polymer Physics* (World Scientific, Singapore, 1995) (`http://www. physik.fu-berlin. de/~kleinert/b5`).

[8] See Appendices of Chapter 3 in the textbook [7], and the article by B. Hamprecht and A. Pelster in: *Fluctuating Paths and Fields* - Festschrift Dedicated to Hagen Kleinert on the Occasion of his 60th Birthday, Eds. W. Janke, A. Pelster, H.-J. Schmidt, and M. Bachmann (World Scientific, Singapore, 2001), p. 347.

[9] Mathematica notebook can be downloaded from `http://www.physik.fu-berlin.de/~kleinert/b5/pgm15`.